

# Theoretical and Experimental Analysis on Thermoelectric Cooling Devices

Michele Anatone\* and Roberto Cipollone†  
*University of L'Aquila, 67100 L'Aquila, Italy*

**The prediction of the performance of Peltier cells as cooling devices is complex inasmuch as it consists of several quite different processes simultaneously present and deeply interrelated (Seebeck and Joule heating effects and conductive and convective heat transfer). However, there are great expectations for these devices for mass production, mainly as air conditioning units for fixed or vehicles onboard application. The advantages with respect to the conventional solutions appear to be even more important. A model that predicts the performance of a Peltier module for cooling applications is presented. An experimental activity demonstrates the validity of the model and its capability as a design tool.**

## Nomenclature

$A$	=	cross-sectional area
$a_{0,1,2}$	=	coefficients
$I$	=	current
$k$	=	thermal conductivity
$L$	=	semiconductor length
$N$	=	total number
$Q$	=	heat flux
$R$	=	electric resistance
$T$	=	temperature
$t$	=	time
$V$	=	voltage
$x$	=	abscissa
$\alpha$	=	Seebeck coefficient
$\rho$	=	electric resistivity

## Subscripts

air	=	bulk conditions
$c$	=	cold junction
cs	=	cold surface
$h$	=	hot junction
hs	=	hot surface
$i$	=	junctions
is	=	internal surfaces
$J$	=	Joule heating
$j$	=	semiconductors
$m$	=	mean
$n$	=	n-type semiconductor
$p$	=	p-type semiconductor
$S$	=	Seebeck
sc	=	semiconductor

## Introduction

**T**HERMOELECTRIC cooling (TEC), based on the Peltier effect, has very interesting capabilities with respect to conventional cooling systems.<sup>1</sup> The absence of moving components results in an increase of reliability, a reduction of maintenance, and an increase of system life; the modularity allows for the application in a wide-scale range without significant losses in performance; the absence of a working fluid avoids environmental dangerous leakage; and the noise reduction appears also to be an important feature.

Moreover, the intrinsic behavior of TEC devices allows for the control of the heat load and of the temperatures of the system to be cooled that are strictly proportional to the applied voltage. This feature appears to be particularly interesting if compared to the inefficiencies of conventional refrigerating systems for partial loading behavior. Because of these advantages, it is expected that interest in TEC systems will increase in those sectors where the environmental pollution and performance at partial loading appear to be more important. This is the case, for instance, of the vehicle's conditioning units where the working conditions are critical for a conventional system (on-off control, weights, oversized components, etc.).<sup>2</sup>

In spite of these advantages, the diffusion of TEC results are limited due to the low coefficient of performance (COP) values that can be reached through the present-day technology. TEC applications are restricted to particular fields where the cooling power is low ( $\sim 100$  W per module), and system miniaturization and high precision in temperature control are the design key factors (laboratories, electronic components, space, etc.).<sup>3</sup> The possibility of increasing the areas of application of TEC devices, in terms of COP and cooling power, are mainly related to the materials and the design of the overall system.<sup>4</sup>

For the improvement of the material properties, increase of the Seebeck coefficient and reductions in the thermal conductivity and the electric resistivity are particularly significant. The science and technology of materials promises performance that seems to increase continuously for other applications (semiconductor science, electronics, etc.).<sup>5,6</sup> The availability of a complete model that considers, from an engineering point of view, all of the processes occurring in a Peltier cell is still far from being achieved. The simulation of the Peltier effect and that of Joule heating, deeply interrelated with a heat transfer problem (conduction inside the semiconductors and convection with the environment), is characterized by great complexity; the spatial distribution of these effects is also important for optimization of performance. This requires distributed parameter models that must be specifically conceived for design tools.

In the literature, the modeling of thermoelectric systems aimed at design has been performed following simplified procedures based on lumped parameters approaches<sup>7–13</sup> that can be suitable for the applications for which the TEC systems are currently used. For these applications, for instance, the geometries of the cells are quite simple (normally all of the thermoelements are distributed on single or stratified planes): This will produce heat transfer situations that can be easily predicted. In spite of this, from a pure theoretical point of view, the Peltier effect has been the subject of intense studies to discern the interior physics of the process.<sup>14,15</sup>

In this paper, a design tool for TEC devices is presented. It is based on a finite element model of different thermoelectric modules with any thermal and electric connection (in series, in parallel, and mixed). The model allows for the evaluation of the steady and

Received 11 May 2000; revision received 25 October 2000; accepted for publication 26 October 2000. Copyright © 2001 by Michele Anatone and Roberto Cipollone. Published by the American Institute of Aeronautics and Astronautics, Inc., with permission.

\*Associate Professor, Department of Energetics.

†Full Professor, Department of Energetics.

unsteady thermal fields inside the module, starting from the voltage applied, and considers the material nonlinearities as well as the true geometry and disposition of the cells inside the module. Heat fluxes exchanged between the cells, therefore, can be evaluated, as well as the relative COP. Because of this feature, the model allows for optimization according to different optimum criteria (maximum heat flux, maximum COP, maximum temperature difference, minimum space for a given application, etc.). A first experimental activity has been performed to assess the validity of the model. The performance of a commercial Peltier module have been predicted with a high degree of accuracy.

### Model

A TEC device is a sequence of elementary cells that can be represented as shown in Fig. 1. Two n-type and p-type semiconductors are electrically connected by means of two junctions. Two ceramic plates (electrically insulator and thermally conductive) separate the single cell from the environment (or from other cells). Supplying a continuous voltage to the cell, the junction at the n-p transition behaves like a heat sink,  $Q_c$ , and in the p-n transition, a heat source,  $Q_h$ , is produced. Because of  $Q_c$ , the temperature at the cold junction  $T_c$  reduces, and a heat flux at the surface  $Q_{cs}$  is drained.  $Q_h$  produces an increase of the hot-junction temperature  $T_h$  so that the heat flux  $Q_{hs}$  is reversed.  $Q_h$  and  $Q_c$  are related to the Seebeck coefficients  $\alpha_n$  and  $\alpha_p$  of the semiconductors, to  $T_h$  and  $T_c$ , and to the electric current  $I$  flowing through the semiconductors and the junctions according to

$$Q_c = [\alpha_n(T_m) - \alpha_p(T_m)]T_c I \quad (1a)$$

$$Q_h = [\alpha_p(T_m) - \alpha_n(T_m)]T_h I \quad (1b)$$

Here,  $\alpha_n$  and  $\alpha_p$  depend on the mean temperature of the semiconductors, evaluated as  $T_m = (T_h + T_c)/2$ .

The electric current depends on the applied voltage  $V$ , on the Seebeck voltage  $V_S$ , which opposes the current, and on the electric resistance of the cell  $R$ :

$$I = (V - V_S)/R \quad (2)$$

with

$$V_S = \int_{T_c}^{T_h} [\alpha_p(T) - \alpha_n(T)] dT \quad (3)$$

$$R = \frac{2}{A_{sc}} \int_0^L \rho_{sc}(T) dx \quad (4)$$

In Eq. (4), the electric resistance of the junctions has been neglected, because their resistivities are about three orders of magnitude smaller than that of the semiconductors. To  $Q_c$  and  $Q_h$ , the Joule heating effect that results distributed inside the semiconductors must be added ( $Q_J = RI^2$ ).

Models currently available in the literature, having an engineering approach, fall in the class of lumped parameters and consider a

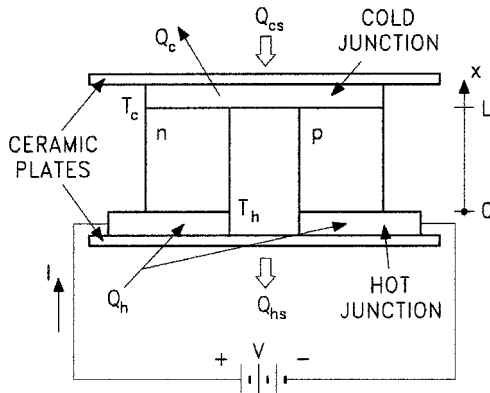


Fig. 1 Elementary Peltier cell.

heat source at the module hot side and a heat sink at the cold side as the boundary conditions between the fluids and the module surfaces. The thermal fluxes derived from Eqs. (1a) and (1b), with the contribution of the Joule heating effect subdivided into two equal parts, are applied to the module sides through a convective heat transfer process. The approach easily leads to the evaluation of the thermal field inside the module and, then, to the Peltier and the Joule heating effects starting from the hot and cold fluids temperatures.<sup>7,8,11,12</sup> In this way several limitations are introduced:

1) The module (semiconductors, electric connections, ceramic plates, etc.) is considered in a one-dimensional context, neglecting the effects of the real geometry on the thermal field (edge effects, air gaps among the inner surfaces, different heat transfer situations, etc.).

2) The Peltier and the Joule heating effects are concentrated on the surfaces facing the hot and the cold fluids; in reality they are distributed inside the module according to the real position of the thermoelectric materials and to the electric resistivity of the different elements inside it.

3) The Peltier effect in terms of  $Q_c$  and  $Q_h$  cannot be considered as boundary conditions, as in the literature, occurring inside the module across the thermoelectric junctions; the presence of the equivalent heat sources and sinks inside the module leads to temperature levels at the boundaries that produce a net (convective) heat transfer between hot and cold fluids.

In this paper these limitations have been overcome, producing a more effective approach in the modeling of TEC modules: The real geometry and disposition of the different materials have been accounted for, as well as the thermoelectric and Joule heating effects being located where they actually take place. The different heat transfer situations across the module surfaces have been considered, discerning between forced and natural convection on vertical and horizontal plates. To take into account these effects, a finite element model has been developed using a commercially available code as a mathematical solver.

In Fig. 2, the finite element model of a Peltier cell is shown: It can be considered as representative of a portion of a TEC module composed of a number of cells connected electrically in series and thermally in parallel. The location of the ceramic plates, of the electric junctions, and of the semiconductors is presented: In this way, the different thermophysical properties can be accounted for. The n-type ( $j-1$ ) and p-type ( $j$ ) semiconductors are welded to the cold junction ( $i$ ). The p-type ( $j$ ) and the next n-type ( $j+1$ ) semiconductors form the hot junction ( $i+1$ ). The Peltier effect is represented in terms of heat flux sinks and sources given by

$$Q_{c,i} = -(\alpha_{j-1}T_{c,j-1} + \alpha_j T_{c,j})I \quad (5a)$$

$$Q_{h,i+1} = +(\alpha_j T_{h,j} + \alpha_{j+1} T_{h,j+1})I \quad (5b)$$

where  $\alpha_j = \alpha(T_{m,j}) = [\alpha_p(T_{m,j}) + |\alpha_n(T_{m,j})|]/2$  and  $T_{m,j} = (T_{h,j} + T_{c,j})/2$ .

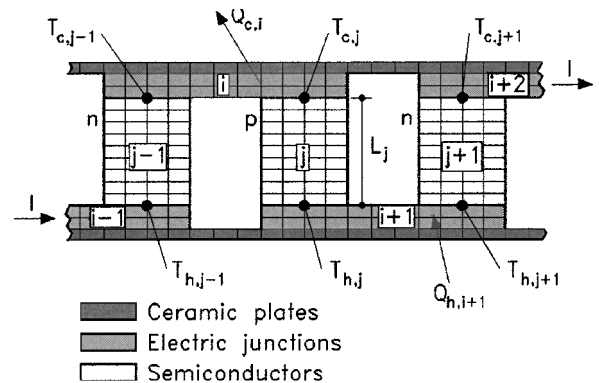


Fig. 2 Finite element model of a Peltier cell.

The temperature values ( $T_{c,j-1}$ ,  $T_{c,i}$ ,  $T_{c,j+1}$ ,  $T_{h,j-1}$ ,  $T_{h,i}$ ,  $T_{h,j+1}$ ) at the semiconductors cold and hot sides are evaluated as mean values on the surfaces between the electric junctions and the semiconductors; the temperature of a semiconductor  $T_{m,j}$  is evaluated as a mean value on its overall volume.  $Q_c$  and  $Q_h$  are located inside the module, in the finite elements that represent the electric junctions, uniformly distributed like heat terms per unit of volume.

The current  $I$  in Eqs. (5a) and (5b) is evaluated according to Eq. (2), where

$$V_S = \sum_{j=1}^{N_{sc}} \alpha_j \Delta T_j \quad (6)$$

$$R = \sum_{j=1}^{N_{sc}} R_j = \sum_{j=1}^{N_{sc}} \rho_{sc,j} \frac{L_j}{A_j} \quad (7)$$

with  $\Delta T_j = T_{h,j} - T_{c,j}$  and  $\rho_{sc,j} = \rho(T_{m,j})$ . In this way, the contributions due to the different materials have been taken into account, as well as all of the terms that influence the electric resistance. Once  $I$  is known, the Joule heating effect  $Q_{J,j} = R_j I^2$  is applied in each semiconductor finite element.

Equations (5a), (5b), (6), and (7) can be reformulated to represent the relative processes occurring inside TEC modules, where single cells are connected anyway from the electric and thermal points of view, as well as for different geometrical configurations. This feature is particularly useful for design purposes because it allows for the optimization of several working parameters of the TEC, such as temperature differences between hot and cold external surfaces, COP, heat fluxes, and so on. This allows also for representing distribution of cells filling complex geometries to fulfill given space constraints.

The thermal field inside the cells has been calculated solving the Fourier equation where heat sinks and source terms have been introduced inside the corresponding elements. As known, this computation is not straightforward because the problem is strongly nonlinear, where these nonlinearities are spread inside each finite element. In this procedure, the calculation starts from an open circuit condition with the module in thermal equilibrium with the surroundings. Voltage is then applied, and an initial current starts to circulate through the cells following Ohm's law, with the Seebeck voltage  $V_S$  equal to zero due to the uniformity in temperatures. The sink and source terms are evaluated by Eqs. (5a) and (5b) and are applied to each element of the junctions. Joule heating is also applied to the elements of the semiconductors. A new thermal field is then calculated, and the thermoelectric material properties are evaluated as a function of the new temperatures, leading to the Seebeck voltage equation (6), to the electric resistance equation (7), and then to the electric current equation (2). The new value for  $I$  determines changes in  $Q_c$ ,  $Q_h$ , and  $Q_J$ , whose upgraded values are applied to the next time step. This explicit numerical scheme corresponds to the need for a suitable choice for the time-space grid.

To reproduce the real heat transfer situations at the boundaries, this model introduces a detailed description, which considers the following:

- 1) Natural convection is specified for vertical or horizontal surfaces, facing upward and downward. This heat transfer usually applies inside the module.
- 2) There is forced convection when the hot and cold fluids are directly facing the ceramic plates.
- 3) Finned plates are present as additional components in thermal contact with the ceramic surfaces. In this case, the geometry of the module increases in complexity, and a suitable heat transfer coefficient (natural or forced convection) is applied on the surfaces facing the environment. Appendix A lists the correlation used for the evaluation of the heat transfer coefficients.

## Results

The model has been detailed for a commercially available TEC module, produced by Melcor (Model CP2-127-06L), with the following characteristics:  $V_{max} = 15.4$  V,  $I_{max} = 14$  A,  $Q_{cs, max} = 120$  W,

$\Delta T_{s, max} = 67^\circ\text{C}$ , values referred to a hot-side surface temperature equal to  $T_{hs} = 25^\circ\text{C}$ . The module is composed of 127 elementary cells (Fig. 1) and has dimensions 62 mm in width, 62 mm in length, and 4.6 mm in thickness. All of these cells are mounted on a layer that results in being electrically in series and thermally in parallel. The TEC module has been represented with 3200 elements; the temperatures are evaluated on 6700 nodes. The semiconductor thermoelectric properties have been computed as function of the temperature (see Appendix B).

To evaluate the validity of the model, an experiment has been carried out with the following boundary conditions applied to the external plates: case A, with natural convection on both surfaces, and case B, with fixed temperature on the hot surface and natural convection on the cold surface.

For case A, the module has been suspended in air. The fluid bulk temperature has been varied from the room conditions (about  $20^\circ\text{C}$ ) to  $0^\circ\text{C}$ . Case B has been obtained by facing the hot surface on a block of steel with a suitable mass representing a high thermal capacity able to keep the temperature constant independent of the heat flux received from the module.

From the theoretical point of view, the boundary conditions applied to the model to reproduce the situations A and B refer to the correlations for natural convection for vertically disposed planes (see Appendix A). The natural convection among the elementary cells has also been accounted for, differentiating between horizontal and vertical surfaces according to Appendix A. The two hot and cold surfaces have been instrumented by means of five k-type thermocouples disposed in a way as to give a mean temperature value on each surface.

The following test procedure has been adopted: Starting from an equilibrium thermal condition, the module is supplied with a voltage step variation until a steady thermal state is obtained. The voltage is then removed. Figures 3a–3d show, for experimental conditions A, a comparison between the theoretical and the experimental temperature on the hot and cold sides of the Peltier module. Figures 3a and 3b refer to two constant voltage supplies equal to 1 and 1.9 V. The initial temperatures of the module are  $22.2^\circ\text{C}$  for Fig. 3a and  $23.6^\circ\text{C}$  for Fig. 3b. At  $t = 0$  s, the voltage step variation is applied up to  $t = 1500$  s, where the temperatures of the two junctions are in equilibrium; then the voltage is removed. The agreement is quite satisfactory during the first temperature transients, during the reaching the equilibrium state, and during the transient that follows the cooling of the two surfaces after switching off the voltage. The maximum temperature differences are less than  $1^\circ\text{C}$ , which guarantees a precision quite satisfactory for design purposes. This is mainly due to the inherent uncertainties of the heat transfer coefficients for natural convection given by the correlations (A1–A5) (see Appendix A). These differences are also of the order of magnitude of those introduced by the sensor placement.<sup>16</sup> The agreement is kept also when the initial temperature of the module is decreased to  $7.4^\circ\text{C}$  (Fig. 3c) and to  $0.4^\circ\text{C}$  (Fig. 3d).

In these experimental situations, the two surfaces reach temperatures above the ambient value. This means that the overall behavior of the module is as a heating device at two temperature levels. Figure 4 shows, for these testing situations, the heat balance at equilibrium. The Joule heating effect  $Q_J$  and the Peltier effect  $Q_h$  at the hot junction dominate over the Peltier effect  $Q_c$  at the cold junction thus producing heat fluxes on the surfaces toward the environment. Figure 4 shows the thermal heat fluxes exchanged by convection through the hot surface  $Q_{hs}$ , the cold surface  $Q_{cs}$ , and the internal module surface  $Q_{is}$ .

Note that, after the voltage is switched off, the overall module behaves like an equivalent thermocouple whose two thermoelements are at different temperature (the values of equilibrium). This physically produces a positive Seebeck voltage  $V_S$  at the module clips, which decreases up to zero as the temperature difference decreases. This phenomenon takes place for the first 30 to 40 s after the voltage switching off. Figures 5a and 5b show the comparison between theoretical [Eq. (6)] and experimental data on  $V_S$  as a function of time, measured after the voltage is switched off. The agreement displayed is quite good, considering the critical conditions of the

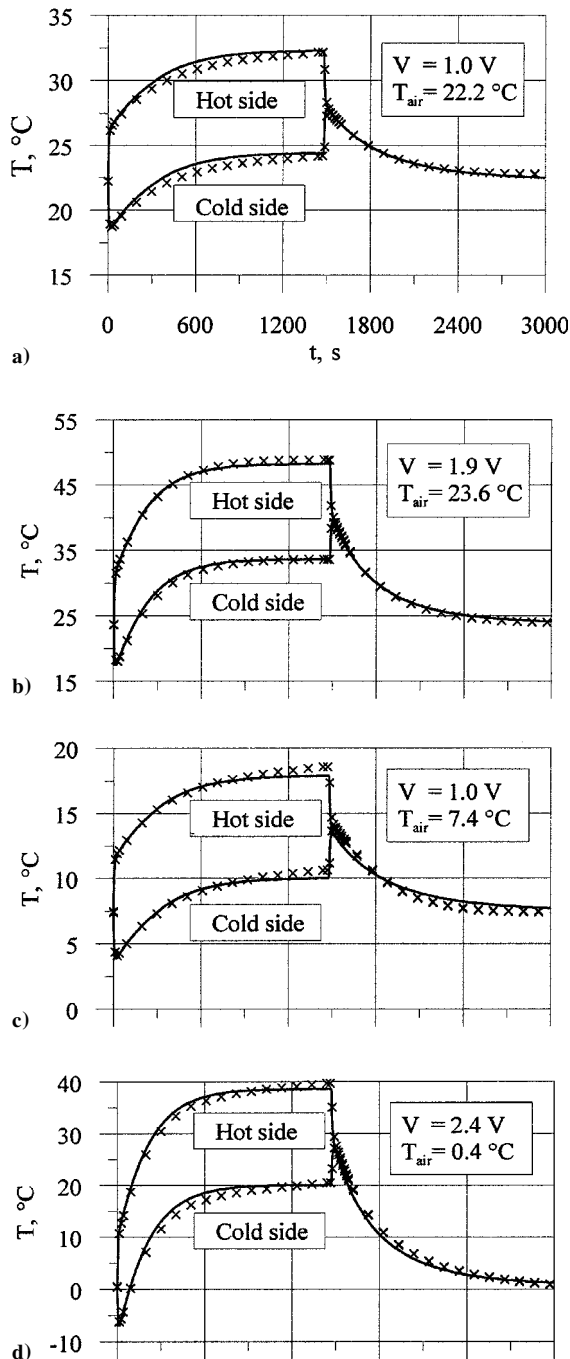


Fig. 3 Theoretical — and experimental  $\times$  surface temperature as a function of time, case A.

comparison:  $V_s$ , as earlier described, is always present during the feeding of the module, and it becomes the dominant electric effect when the module is switched off.

When the temperature at the hot side is kept constant (experimental situation described as case B), the behavior of the module becomes correct: Figures 6a–6c show the temperature at the cold side, produced by a voltage variation, which remains constant for 300 s and then returns to zero. The three situations refer to three voltage supplies (0.5, 1, and 1.5 V). The cold side cools and reaches a steady value after a shorter period (with respect to the preceding case).  $Q_J$ ,  $Q_c$ , and  $Q_h$  rearrange in a way to produce a net cooling effect  $Q_{cs}$ .  $Q_{hs}$  is completely absorbed by the hot surface, kept at constant temperature.

Figure 7a gives the net cooling effect  $Q_{cs}$  as a function of the supplied voltage: The variation shows significant dependence. The same considerations apply to the COP (Fig. 7b). The data reported

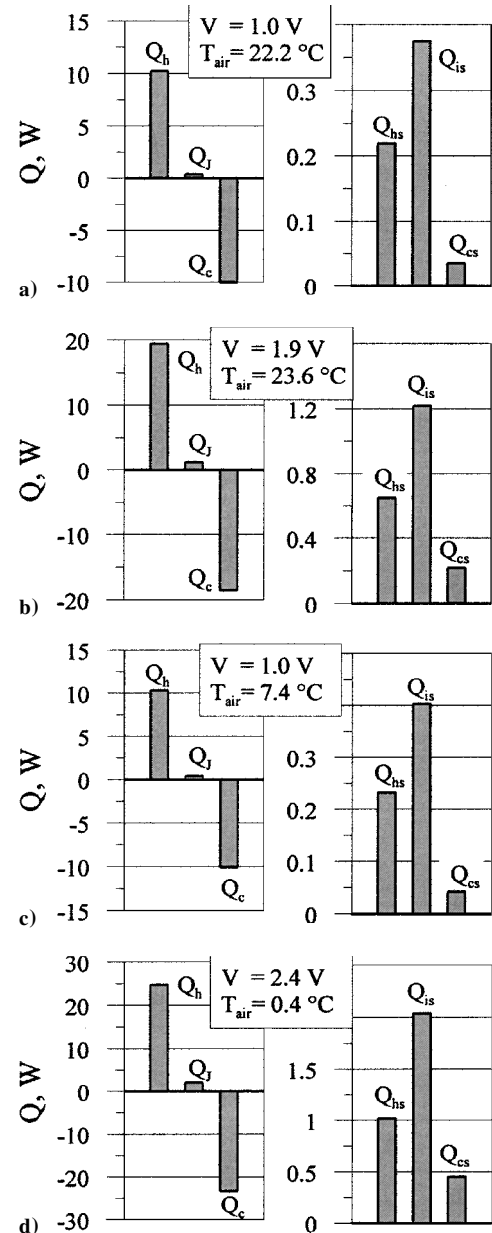


Fig. 4 Generated and exchanged heat fluxes, case A.

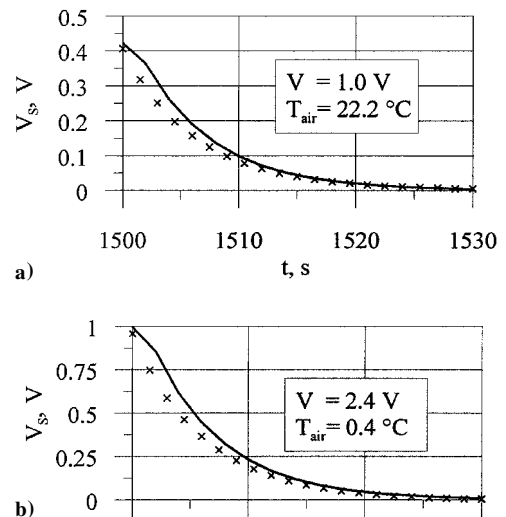


Fig. 5 Theoretical — and experimental  $\times$  Seebeck voltage as a function of time, case A.

Table B1 Thermoelectric properties as a function of temperature

Parameter	Coefficient $a_0$	Coefficient $a_1$	Coefficient $a_2$
$\alpha$	$2.22 \times 10^{-5}$ , V/K	$9.30 \times 10^{-7}$ , V/K <sup>2</sup>	$-9.91 \times 10^{-10}$ , V/K <sup>3</sup>
$\rho$	$5.11 \times 10^{-7}$ , $\Omega\text{m}$	$1.63 \times 10^{-8}$ , $\Omega\text{m/K}$	$6.28 \times 10^{11}$ , $\Omega\text{m/K}^2$
$\kappa$	6.26, W/mK	$-2.78 \times 10^{-2}$ , W/mK <sup>2</sup>	$4.13 \times 10^{-5}$ , W/mK <sup>3</sup>

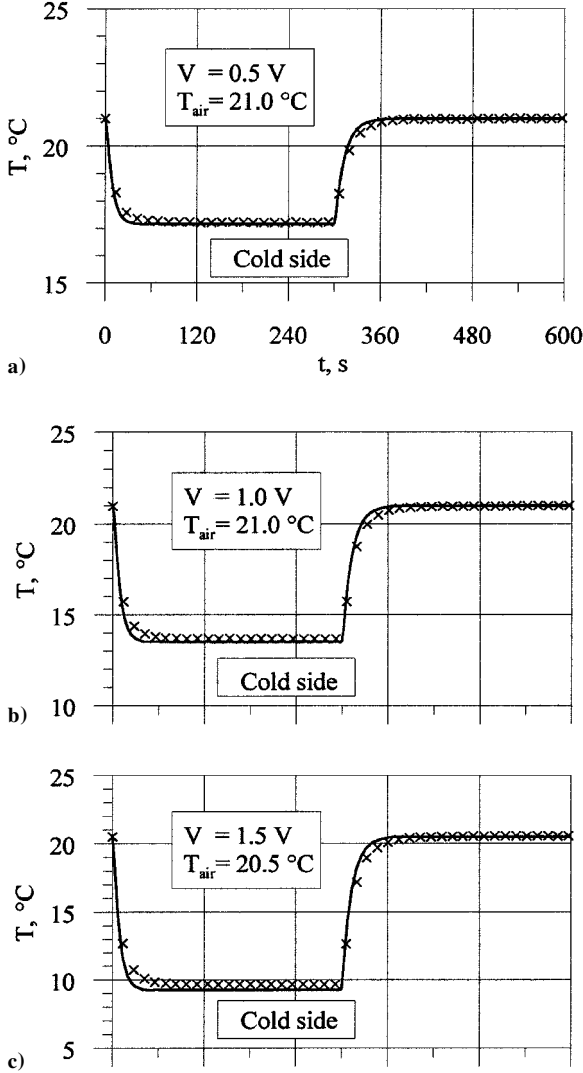


Fig. 6 Theoretical — and experimental × surface temperature as a function of time, case B.

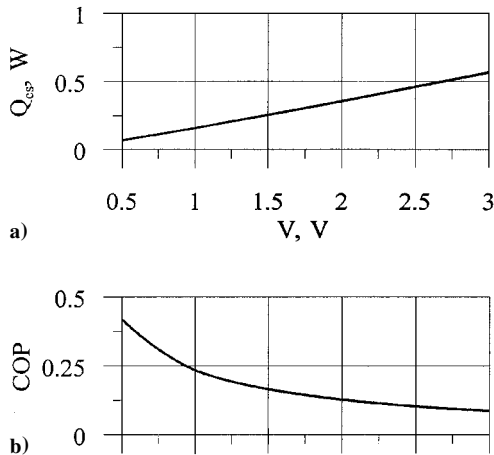


Fig. 7 Cooling effect and COP as a function of the voltage, case B.

in Figs. 4 and 7 are calculated from the model when equilibrium is reached: These values match the experimental data very closely because of the good agreement obtained on the temperatures, which represents a much more critical test.

To evaluate the influence of the numerical aspects related to the solution procedure, all of the presented predictions have been repeated, varying the time-space grid. When the module is represented with 38,000 elements, maximum temperature differences of 0.2 °C are found, meaningless for design purposes if one also considers the computing time increases of one order of magnitude. A still lower influence is associated with the integration time step.

### Conclusions

The simulation of the behavior of a TEC device requires the modeling of many different processes strictly linked with each other. In this problem, the real geometry of the module, the spatial distribution of the different materials inside the elementary cells, and the heat transfer situations at the boundary strongly influence the thermal processes and must be accounted for.

In this paper a new modeling aimed at the design of TEC devices has been presented. It is based on a finite element formulation of the complex thermal problems occurring, which allows for the fore-mentioned aspects to be accounted for. An experimental test bed has been built to validate the effectiveness of the model that has been used to reproduce the behavior of a commercial TEC module. Transient tests have been designed to verify the capability of the model in predicting subprocesses (Seebeck effect) or abnormal situations, where the module behaves like a heat source, producing a net heating.

Comparisons have been made in terms of temperatures on the external surfaces: The agreement is quite satisfactory (in the worst case a difference of about 1 °C is found), and this aspect ensures the accuracy in the prediction of the heat flows exchanged.

The model has been conceived to predict the performance of unconventional arrangements among single elementary cells from the electrical and thermal points of view, in series, in parallel, and in mixed configurations.

Although the model has been conceived as a design code for TEC devices, because of its strict physical consistency, it appears eligible as a predicting tool of the performance of more general devices based on the Peltier effect.

### Appendix A: Correlations for the Heat Transfer Coefficient

The natural convection heat transfer coefficient has been calculated through the following nondimensional relationships.

For vertical surfaces,<sup>17</sup>

$$Nu = 0.68 + \frac{0.67(Gr Pr)^{\frac{1}{4}}}{[1 + (0.492/Pr)^{\frac{9}{16}}]^{\frac{4}{9}}} \quad (A1)$$

for  $Gr Pr < 10^9$  and

$$Nu = 0.83 + \frac{0.39(Gr Pr)^{\frac{1}{4}}}{[1 + (0.492/Pr)^{\frac{9}{16}}]^{\frac{8}{27}}} \quad (A2)$$

for  $10^9 < Gr Pr < 10^{12}$ .

For horizontal surfaces facing upward,<sup>18</sup>

$$Nu = 0.13 + (Gr Pr)^{\frac{1}{3}} \quad (A3)$$

for  $GrPr < 2 \times 10^8$  and

$$Nu = 0.16 + (GrPr)^{\frac{1}{3}} \quad (A4)$$

for  $2 \times 10^8 < GrPr < 10^{11}$ .

For horizontal surfaces facing downward,<sup>18</sup>

$$Nu = 0.58 + (GrPr)^{\frac{1}{3}} \quad (A5)$$

for  $10^6 < GrPr < 10^{11}$ .

## Appendix B: Semiconductor Thermoelectric Properties

The semiconductors' thermoelectric properties have been evaluated, as a function of the temperature, by means of parabolic relationships, in the form  $a_0 + a_1 \cdot T + a_2 \cdot T^2$ , with the coefficients reported in Table B1.<sup>19</sup> At 298 K, values from Table B1 give  $\alpha = 211.6 \mu\text{V/K}$ ,  $\rho = 1.096 \times 10^{-5} \Omega\text{m}$ , and  $k = 1.654 \text{ W/mK}$ . The semiconductors density has been assumed equal to  $7500 \text{ kg/m}^3$ , according to Ref. 19.

## References

- <sup>1</sup>Goldsmid, H. J., "Application of Thermoelectric Cooling," *CRC Handbook of Thermoelectrics*, CRC Press, Boca Raton, FL, 1995, pp. 617–620.
- <sup>2</sup>Stockholm, J. G., "Large-Scale Cooling: Integrated Thermoelectric Element Technology," *CRC Handbook of Thermoelectrics*, CRC Press, Boca Raton, FL, 1995, pp. 657–666.
- <sup>3</sup>"Peltier Effect Technology and Applications," National Technical Information Service, Springfield, VA, Jan. 1998.
- <sup>4</sup>Stockholm, J. G., "Current State of Peltier Cooling," *16th International Conference on Thermoelectrics*, IEEE Publications, Piscataway, NJ, 1997.
- <sup>5</sup>Krainak, M., Abshire, J., Cornwell, D., Dragic, P., Duerksen, G., and Switzer, G., "Research and Development of Laser Diode Based Instruments for Applications in Space," *Space Technology and Applications International Forum*, American Institute of Physics, College Park, MD, 1999.
- <sup>6</sup>"Electrochemical Characterization of Semiconductor Materials and Structures," Dept. of Electrical Engineering, Cleveland State University, TR CR303094, Cleveland, OH, Feb. 1997.
- <sup>7</sup>Stockholm, J. G., and Stockholm, D. W., "Thermoelectric Modeling of a Cooling Module with Heat Exchangers," *11th International Conference on Thermoelectrics*, IEEE Publications, Piscataway, NJ, 1992.
- <sup>8</sup>Stockholm, J. G., "Modeling of Thermoelectric Cooling Systems," *CRC Handbook of Thermoelectrics*, CRC Press, Boca Raton, FL, 1995, pp. 677–686.
- <sup>9</sup>Taylor, P. J., "Model for the Non-Steady-State Temperature Behaviour of Thermoelectric Cooling Semiconductor Devices," *Semiconductor Science and Technology*, Vol. 12, No. 4, 1997, pp. 443–447.
- <sup>10</sup>Min, G., and Rowe, D. M., "Improved Model for Calculating the Coefficient of Performance of a Peltier Module," *Energy Conversion and Management*, Vol. 41, No. 2, 2000, pp. 163–171.
- <sup>11</sup>Buist, R. J., "Calculation of Peltier Device Performance," *CRC Handbook of Thermoelectrics*, CRC Press, Boca Raton, FL, 1995, pp. 143–156.
- <sup>12</sup>Lau, P. G., and Buist, R. J., "Temperature and Time Dependent Finite-Element Model of a Thermoelectric Couple," *15th International Conference on Thermoelectrics*, IEEE Publications, Piscataway, NJ, 1996.
- <sup>13</sup>Buist, R. J., and Lau, P. G., "Theoretical Analysis of Thermoelectric Cooling Performance Enhancement via Thermal and Electric Pulsing," *15th International Conference on Thermoelectrics*, IEEE Publications, Piscataway, NJ, 1996.
- <sup>14</sup>Pollok, D. D., *Physics of Engineering Materials*, Prentice Hall, Englewood Cliffs, NJ, 1990, Chap. 2.
- <sup>15</sup>Bridgeman, P. W., *The Thermodynamics of Electrical Phenomena in Metals*, Dover, New York, 1961, Chap. 3.
- <sup>16</sup>Anatone, M., and Cipollone, R., "Some Considerations on the Precision of the Temperature Measurement in Thermal Machines Components," *44th Italian National Congress of the Associazione Termotecnica Italiana*, McGraw-Hill, New York, 1989, (in Italian).
- <sup>17</sup>Holman, J. P., *Heat Transfer*, McGraw-Hill, New York, 1989, Chap. 7.
- <sup>18</sup>Churchill, S. W., and Chu, H. H. S., "Correlating Equations for Laminar and Turbulent Free Convection from a Vertical Plate," *International Journal of Heat and Mass Transfer*, Vol. 18, 1975, pp. 1323–1329.
- <sup>19</sup>*Thermoelectric Handbook*, Melcor Co., Trenton, NJ, 2000.